Cell Reports

Clusters of Tolerogenic B Cells Feature in the Dynamic Immunological Landscape of the Pregnant Uterus

Graphical Abstract

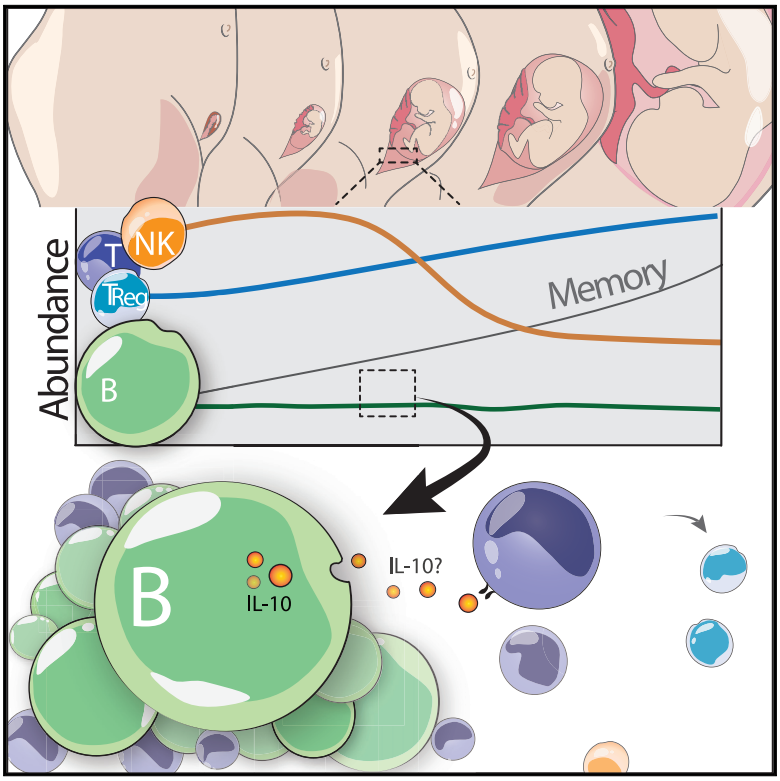

Authors

Marilen Benner, Dorien Feyaerts, Celia Cartagena García, ..., Irma Joosten, Gerben Ferwerda, Renate G. van der Molen

Correspondence

marilen.benner@radboudumc.nl (M.B.), renate.vandermolen@radboudumc.nl (R.G.v.d.M.)

In Brief

Benner et al. present a detailed analysis of the immune dynamics at the fetal-maternal interface throughout human gestation, revealing that B cells with a unique phenotype are a notable presence during healthy pregnancy. This may suggest a regulatory mechanism contributing to the local immune environment.

Highlights

- B cells obtained from the fetal-maternal interface gain memory during gestation
- Unsupervised analysis shows B cell subsets with marker expression unique to the uterus
- Decidual B cells are able to secrete IL-10
- Clusters of decidual B cells also contain T cells, including Foxp3^{pos} T cells

Benner et al., 2020, Cell Reports *32*, 108204
September 29, 2020
https://doi.org/10.1016/j.celrep.2020.108204

CellPress

Cell Reports

CellPress
OPEN ACCESS

Report

Clusters of Tolerogenic B Cells Feature in the Dynamic Immunological Landscape of the Pregnant Uterus

Marilen Benner,[1,*] Dorien Feyaerts,[1,5] Celia Cartagena García,[1,6] Nurcan Inci,[1] Sergi Cedó López,[1] Esther Fasse,[1] Wijs Shadmanfar,[2] Olivier W.H. van der Heijden,[3] Mark A.J. Gorris,[4] Irma Joosten,[1] Gerben Ferwerda,[1] and Renate G. van der Molen[1,7,*]

[1]Radboud Institute for Molecular Life Sciences, Radboud University Medical Center, Department of Laboratory Medicine, 6500 HB Nijmegen, the Netherlands
[2]MildredClinics Arnhem, 6814 AB Arnhem, the Netherlands
[3]Department of Obstetrics and Gynaecology, Radboud University Medical Center, 6500 HB Nijmegen, the Netherlands
[4]Radboud Institute for Molecular Life Sciences, Department of Tumor Immunology, 6500 HB Nijmegen, the Netherlands
[5]Present address: Department of Anesthesiology, Perioperative and Pain Medicine, Stanford University School of Medicine, Palo Alto, CA 94305, USA
[6]Present address: Beckman Coulter, Life Sciences Research, 13009 Marseille, France
[7]Lead Contact
*Correspondence: marilen.benner@radboudumc.nl (M.B.), renate.vandermolen@radboudumc.nl (R.G.v.d.M.)
https://doi.org/10.1016/j.celrep.2020.108204

SUMMARY

Well-timed interaction of correctly functioning maternal immune cells is essential to facilitate healthy placenta formation, because the uterine immune environment has to tolerate the semi-allogeneic fetus and allow adequate trophoblast invasion. Here, we assess the uterine immune signature before and during pregnancy. Extensive supervised and unsupervised flow cytometry clustering strategies not only show a general increase in immune memory throughout pregnancy but also reveal the continuous presence of B cells. Contrary to the belief that B cells are merely a consequence of uterine pathology, decidual B cells produce IL-10 and are found to be localized in clusters, together with Foxp3^{pos} T cells. Our findings therefore suggest a role for B cells in healthy pregnancy.

INTRODUCTION

The uterus is a highly dynamic compartment. Each cycle, in preparation of pregnancy, the endometrium undergoes decidualization, a complex process of mucosal differentiation and influx of immune cells dictated by changing hormone levels. During the early stages of pregnancy, the well-timed presence of correctly functioning maternal immune cells contributing to both correct trophoblast invasion of semi-allogeneic fetal cells and spiral artery remodeling is essential (Dimitriadis et al., 2005; Mor et al., 2011; Robertson et al., 2011; Robertson and Moldenhauer, 2014). Impairment in the recruitment, induction, or activation of immune components at the fetal-maternal interface can be harmful for mother and/or child. Depending on the nature and timing of the erroneous interactions, (recurrent) miscarriages, preeclampsia (PE), intra-uterine growth restriction, or pre-term labor (PTL) may occur (Mor et al., 2011; Redman and Sargent, 2010; Smith, 2010).

After the initial challenge of implantation, the uterine immune environment faces the task of maintaining an anti-inflammatory state (Mor et al., 2011). Maternal uterine immune cells have to regulate the response to local or systemic infections, counteracting threats to maternal and fetal health while preventing a harmful inflammatory cascade. Any disbalance in the local immune response during this crucial window of development may affect the unborn child, with possible long-term effects on immunity (Hsu and Nanan, 2014; Lasala and Zhou, 2007) or cognitive function (Ashdown et al., 2006; Ratnayake et al., 2013). In the last stage of pregnancy, proinflammatory signaling facilitates physiological uterine contractions through infiltration of leucocytes into the decidua and myometrium and stimulation of cytokine secretion (Shynlova et al., 2013a). In addition, these adaptations may prepare for wound healing and tissue remodeling processes after parturition (Mitchell and Taggart, 2009; Shynlova et al., 2013b).

Although knowledge about the chronology of the systemic immune states during pregnancy has advanced in recent years, studies on gestational uterine immune cell fluxes are scarce (Aghaeepour et al., 2017; Han et al., 2019). Here, we examined local immune cell dynamics throughout human gestation using endometrial lymphocytes derived from menstrual blood alongside decidual tissue from 1st- and 2nd-trimester and term decidua from uncomplicated pregnancies. We provide an overview of lymphocytes present within the uterus throughout gestation, with a focus on B cells with interleukin-10 (IL-10)-secreting capacities.

RESULTS

The Uterus Is a Highly Dynamic Immune Compartment

Onset and maintenance of pregnancy elicit both short-term and long-term adaptations of local immunity to facilitate healthy pregnancy. Thus, we assessed the immune cell composition in human uterine tissues (menstrual blood and decidua) from the non-pregnant phase, to the 1st and 2nd trimesters, and up to term pregnancy using high-dimensional immunophenotyping (Figure 1A). We first examined the abundance of the major lymphocyte cell types in the uterine mucosa over time, using supervised flowcytometric analysis. For menstrual blood mononuclear cells (MMCs), we observed that the natural killer (NK) cell abundance ($CD45^{pos}CD3^{neg}CD56^{pos}$) was relatively higher than in peripheral blood (Figure 1B), as previously shown (Feyaerts et al., 2017; Hosseini et al., 2014). NK cell levels were high in 1st-trimester decidua, stayed at that level in the 2nd trimester, and dropped toward term (Figure 1B). Independent of the time point of gestation, most decidual NK cells were negative for CD16 and showed high expression of CD56 (NK^{bright}, Figure S1C). Compared with peripheral blood, lower T cell ($CD45^{pos}CD3^{pos}CD56^{neg}$) frequencies were seen in MMCs, decreased further in 1st- and 2nd-trimester decidua (Figure 1C), and increased again toward term. In MMCs, the distribution of $CD4^{pos}$ and $CD8^{pos}$ cells within the total $CD3^{pos}$ T cell population was similar to that in peripheral blood (Figure S1D). After initiation of pregnancy, within $CD3^{pos}$ T cells, the frequency of $CD8^{pos}$ cells increased locally and remained at that level throughout pregnancy. $CD4^{pos}$ T cell frequency decreased in 1st-trimester decidua (Figure S1D). Overall abundance of $CD4^{pos}$ T cells within all $CD3^{pos}$ T cells remained relatively low over the course of pregnancy compared with MMCs or peripheral blood. Previously, the percentage of naive $CD4^{pos}$ ($CD45RA^{pos}CCR7^{pos}$) T cells was shown to decrease over the course of pregnancy (Feyaerts et al., 2017). Here, we observed that this switch from naive toward a memory/effector phenotype already takes place at the earliest stage of pregnancy in 1st-trimester decidua (Figures S1E and S1F). A slight drop in $CCR4^{neg}CCR6^{neg}CXCR3^{pos}CD4^{pos}$ T cells (T helper [Th] 1) was observed in 2nd-trimester samples (Figure S1G). $CCR4^{pos}CCR6^{pos}CXCR3^{neg}CD4^{pos}$ (Th17) decreased from 1st trimester to term (Figure S1G). A prominent role in the delicate balance of immunity versus tolerance at the fetal-maternal interface is ascribed to regulatory T (Treg) cells (Tsuda et al., 2019). Compared with peripheral blood ($CD4^{pos}Foxp3^{pos}Helios^{pos}CD25^{Hi}CD127^{low/neg}$, Figure S1H), Treg cell levels in MMCs were low. In pregnancy, levels rose gradually from 1st trimester to 2nd trimester and then remained at this level up to parturition (Figure 1D). Although levels of natural killer T (NKT) cells ($CD45^{pos}CD3^{pos}CD56^{pos}$) in MMCs were similar to those in peripheral blood, their abundance in decidual tissue was highest at term (Figure S1I). Samples of all gestational ages contained a small $CD3^{neg}CD19^{pos}$HLA-DR^{pos} B cell population (Figures 1E and 1F).

To further explore phenotypic features of the different cell populations, we employed an unsupervised approach, using the CITRUS (cluster identification, characterization, and regression) tool on the Cytobank platform. This hierarchical clustering method stratifies cell subtypes based on similar descriptive features (i.e., marker expression) that correlate with the assigned sample type—in this case, gestational age (Bruggner et al., 2014). The six most stratifying clusters to predict gestational age are shown in Figures 1G and 1H. The most predictive clusters were $CD4^{pos}$ T cells (cluster A, $CD45^{pos}CD3^{pos}CD4^{pos}CD8^{neg}$), followed by NK^{bright} (cluster B, $CD45^{pos}CD3^{neg}CD56^{pos}CD16^{neg}$) cells, $CD8^{pos}$ T cells (cluster E, $CD45^{pos}CD3^{pos}CD4^{neg}CD8^{pos}$), and Treg cells (cluster F, $CD45^{pos}CD4^{pos}CD25^{Hi}HLA^{neg}DR^{pos}$). In line with supervised analysis, T cell clusters A, C, E, and F decreased in frequency of overall lymphocytes from MMCs to 1st-trimester decidua and increased toward term, whereas NK cell clusters B and D showed the reverse pattern. Decidual NK cells expressing CD25 (cluster D, $CD45^{pos}CD3^{neg}CD56^{pos}CD25^{pos}CD16^{neg}$), an NK cell subtype suspected to be upregulated because of trophoblast contact at the fetal-maternal interface (Tao et al., 2015), was detected. A cluster representing $CD45^{pos}CD3^{neg}CD19^{pos}$HLA-$DR^{pos}$ B cells was present in both MMCs and decidual tissue at all gestational ages (Figure 1G).

Pregnancy Is Accompanied by a Gain in Decidual B Cell Memory

Having established that B cells are present in decidua throughout pregnancy, we investigated their phenotype in more detail. Little is known on their phenotype within the uterine mucosa. Supervised analysis revealed that similar to peripheral blood, MMC-derived B cells were mainly naive ($IgD^{pos}CD27^{neg}$, Figure 2A). Their frequency was lower upon initiation of pregnancy and dropped further toward the 2nd trimester (Figure 2B). Switched memory B cells ($IgD^{neg}CD27^{pos}$) increased from MMCs throughout gestation (Figure 2C). Abundance of non-switched memory B cells ($IgD^{pos}CD27^{pos}$) was comparable to that in peripheral blood and remained steady during gestation (Figure 2D). The frequency of plasmablasts ($CD27^{pos}CD38^{pos/hi}IgD^{neg}$) was low in MMCs and 1st-trimester decidua compared with peripheral blood (Figure 2E). Plasmablast abundance increased from MMCs to 2nd-trimester and term decidua. The overall frequency of B cells positive for CD27, a memory marker, increased upon pregnancy (Figure 2F) (Klein et al., 1998; Sanz et al., 2008).

Decidual B Cells Are Distinct from Peripheral Blood B Cells

Recent studies emphasize the diversity in B cell subsets, including populations with regulatory capacities (regulatory B [Breg] cells), especially when comparing systemic to tissue-specific immunity (Hasan et al., 2019; Simon et al., 2016). To gain more in-depth insight into B cell subsets in decidual tissues versus peripheral blood, we employed a CITRUS-based, multidimensional, unsupervised clustering analysis. While considered a common B cell marker (Pavlasova and Mraz, 2020), we included CD20 in our clustering analysis for assessment of its possible differential expression. The decidual B cell population contained four subsets that were absent from peripheral blood (clusters I–IV, Figure 3A; marker expression, Figures 3C and 3D): cluster I, comprising $CD24^{hi}CD27^{pos}CD38^{neg}$ cells, and cluster II, comprising $CD24^{pos}CD27^{pos}CD38^{pos}$ cells (cells of both clusters

CellPress
OPEN ACCESS

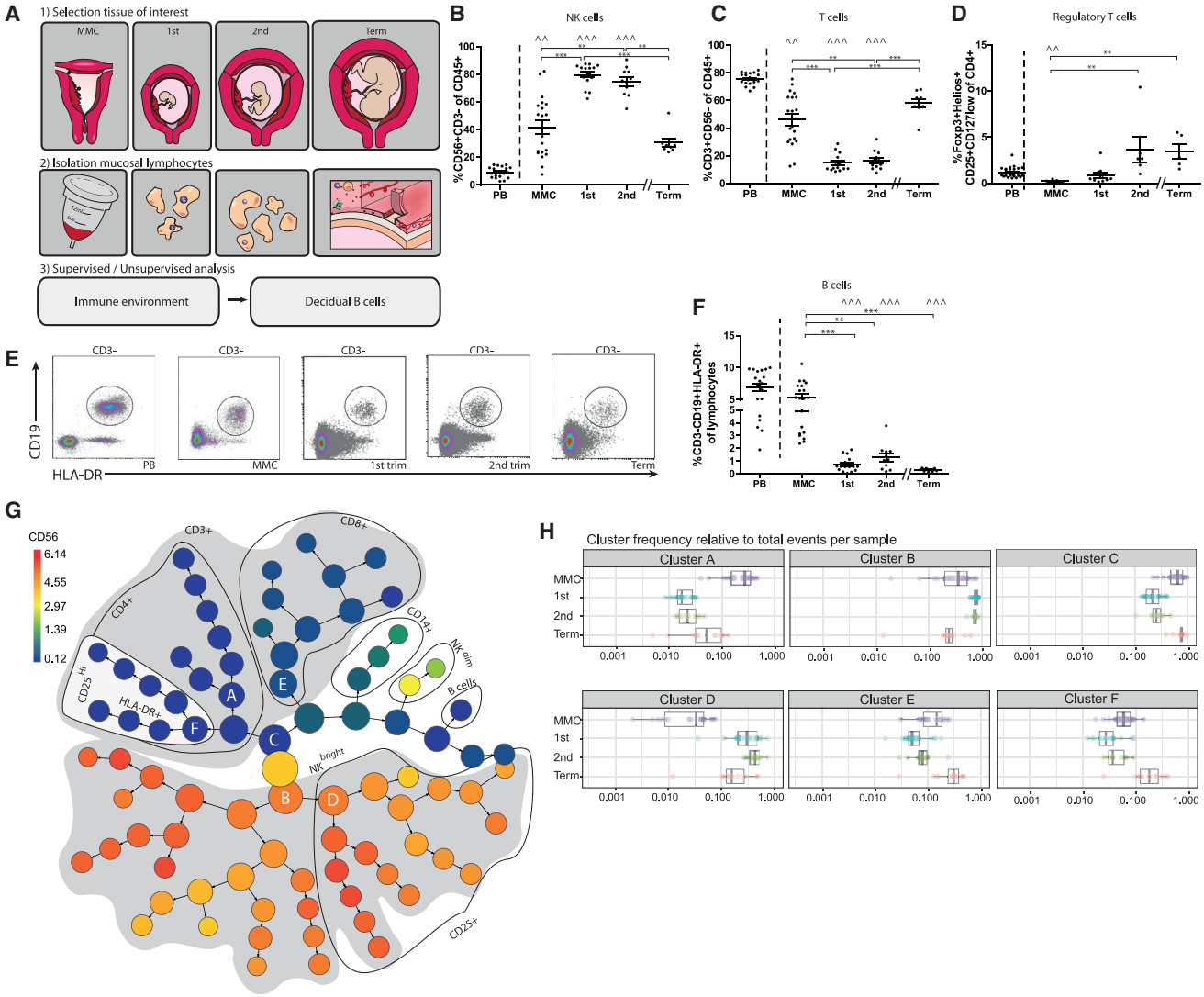

Figure 1. The Dynamic Immune Environment of Mucosal Tissue from Menstrual Blood to Term Decidua

(A) Representation of samples chosen and workflow to study decidual lymphocytes of varying time points in absence of, and during, pregnancy.

(B–D) Frequencies of NK cells (B), T cells (C), and Treg cells (D) in single-cell suspensions. Gating strategies are shown in Figures S1A and S1B. Peripheral blood (PB), n = 20; menstrual blood (MMCs), n = 20; 1st trimester, n = 16; 2nd trimester, n = 11; term pregnancy, n = 9.

(E and F) CD19^{pos} HLA-DR^{pos} B cells could be found in MMCs and 1st-trimester, 2nd-trimester, and term decidua.

(G and H) Stratification of menstrual-blood-derived cells and decidual lymphocytes based on hierarchical clustering using CD3, CD4, CD8, CD14, CD16, CD19, CD25, CD56, and HLA-DR to identify populations of similar marker expression and their abundance using the CITRUS tool by Cytobank. 5,000 events (gating strategy, Figure S2A) were sampled per file, and prediction analysis for microarrays (PAM) clustering was applied to identify clusters contributing to gestational-age-dependent, stratifying signatures (model error rate is shown in Figure S2B). The color scale illustrates the relative marker expression per cluster, whereas the size of each node represents event frequency. As an example, CD56 expression is shown (G), and super-clusters indicate the frequency of each marker per cluster (Figures S2C and S2D). Relative frequency of clusters compared with total lymphocyte count identified as most stratifying is shown for menstrual blood and 1st-trimester, 2nd-trimester, and term decidua samples and ordered from A to F as they decrease in their contribution to stratification (H). Samples of <5,000 lymphocytes were excluded from analysis. MMCs, n = 20; 1st trimester, n = 40; 2nd trimester, n = 16; term pregnancy, n = 9.

^p < 0.05, ^^p < 0.01, ^^^p < 0.001, Kruskal-Wallis and post hoc Dunn's multiple-comparison tests to assess differences between mucosa and PB; *p < 0.05, **p < 0.01, ***p < 0.001, Kruskal-Wallis test to compare MMCs with 1st-trimester, 2nd-trimester, and term decidua. Data are represented as mean ± SEM.

were further characterized as IgD^{low}IgM^{low}CD20^{pos}); cluster III, comprising IgD^{neg}IgM^{low}CD20^{neg}CD24^{hi}CD27^{neg}CD38^{hi} cells; and cluster IV, comprising IgD^{pos}IgM^{low}CD20^{pos}CD24^{pos} CD27^{neg}CD38^{pos} cells (Figure 3A). Cluster III was not observed in term decidua. Two additional clusters were more abundant in peripheral blood: cluster V, resembling plasmablasts (IgD^{neg}IgM^{low}CD20^{neg}CD24^{neg}CD27^{hi}CD38^{hi} cells), and cluster VI (IgD^{pos}IgM^{pos}CD20^{pos}CD24^{low} CD27^{low} CD38^{low} cells) (Figure 3B; marker expression, Figures 3C and 3D).

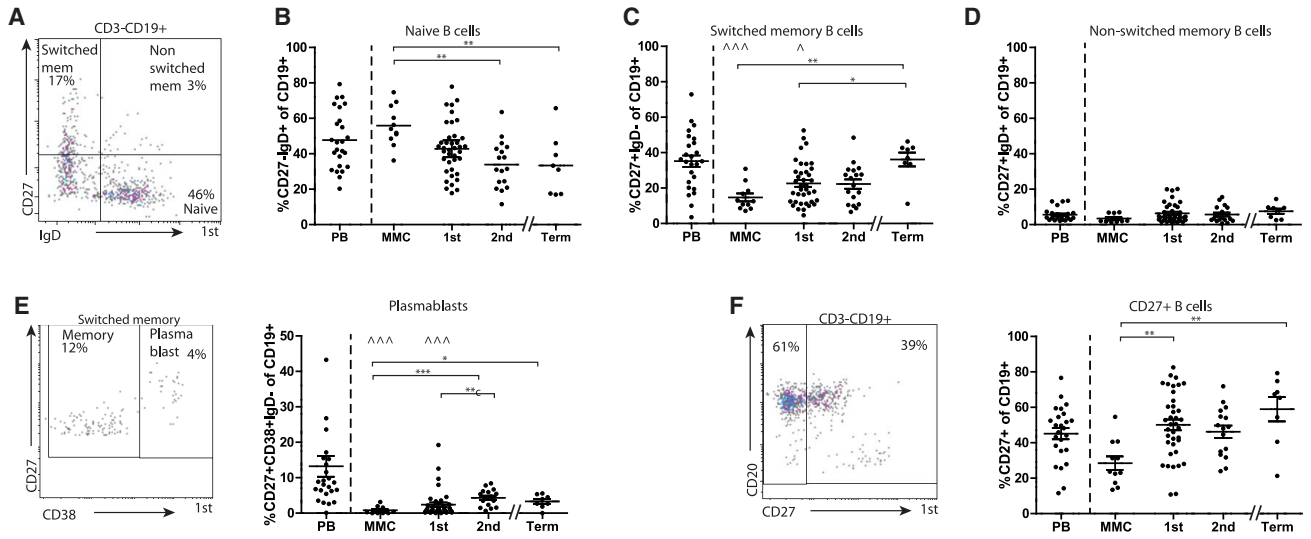

Figure 2. Differential Expression of B Cell Subsets in Samples of Decidua

(A–D) Gating strategy (A) for characterization of naive (B) and switched memory (C) and non-switched memory (D) B cells based on immunoglobulin (Ig) D and CD27 expression (within B cells) (gating strategy, Figure S3A) in PB (n = 25), menstrual blood (MMCs, n = 11), and 1st (n = 39) and 2nd (n = 17) trimesters, as well as term decidua (n = 8).

(E) $CD27^{pos}IgD^{neg}$ cells were further classified as plasmablasts in case of additional CD38 staining.

(F) CD27 positivity of $CD19^{pos}$ B cells.

^p < 0.05, ^^p < 0.01, ^^^p < 0.001, Kruskal-Wallis and Dunn's multiple-comparison tests to assess differences between isolated mucosal tissues and PB; *p < 0.05, **p < 0.01, ***p < 0.001 to compare MMCs and 1st-trimester, 2nd-trimester, and term decidua. Data are shown as mean ± SEM.

Decidual B Cells Have *In Vitro* IL-10-Producing Capacity and Are Found in Clusters

Mouse studies revealed a role for Breg cells in healthy pregnancy (Guzman-Genuino and Diener, 2017; Guzman-Genuino et al., 2019b; Slawek et al., 2020). For human B cells, regulatory properties have been ascribed to several phenotypically distinct B cell subsets, united in their ability to produce IL-10 (Sarvaria et al., 2017). To examine the presence of possible Breg cells in the different decidual tissues, we performed *in vitro* stimulation of decidual and peripheral blood mononuclear cells (PBMCs) in the absence or presence of CpG (TLR9 activation) and CD40L (mimicking T cell-dependent triggering of CD40) (Daien et al., 2014; Iwata et al., 2011). Upon stimulation, higher frequencies of decidua-derived IL-10-expressing B cells compared with peripheral-blood-derived ones were found (Figures 4A and 4B). In the absence of additional CpG and CD40L stimulation, 1st- and 2nd-trimester decidua-derived B cells already expressed IL-10 (Figure 4C).

Information on decidual B cell localization is scarce. Immunohistochemical analysis on 1st- and 2nd-trimester decidua revealed that B cells were located close to T cells (Figure 4D). Because several studies in humans and mice have pointed out the importance of IL-10-secreting B cells for Treg cell induction (Busse et al., 2019; Carter et al., 2011; Flores-Borja et al., 2013; Xing et al., 2015), we investigated whether these decidual lymphocyte clusters also harbored Treg cells. Additional staining of Foxp3, a key transcription factor of Treg cells, showed the presence of $Foxp3^{pos}CD3^{pos}$ T cells close to the B cells (Figures 4E and S3C).

DISCUSSION

Pregnancy poses an immunological challenge, because semi-allogeneic fetal cells have to invade maternal tissue for correct placenta formation. Here, we provide an overview of the dynamic changes in lymphocyte subsets, shaping the gestational immune environment. We highlight a possible role for decidual B cells, whose potential contribution to healthy pregnancy is starting to be considered. Our data reveal that B cells undergo phenotypic adaptations in the decidual tissues over time, which may be regarded as a physiological component of healthy pregnancy.

The possible relevance of B cells for healthy pregnancy is gaining attention (Dutta et al., 2019). In mice, it was shown that the lack of mature B cells is associated with reduced litter size, decreased size of the embryos, and higher susceptibility to prenatal infections (Busse et al., 2019). In women with common variable immunodeficiency, a condition associated with reduced frequencies of switched memory B cells in peripheral blood (Bright et al., 2013), an elevated risk for preterm birth or other pregnancy complications, such as PE, stillbirth, or vaginal bleeding, was observed (Kralickova et al., 2015). Recurrent miscarriage (Carbone et al., 2016; Ota et al., 2014) and PE (Zeng et al., 2013) were linked to alterations in the induction of B cell memory. Although there is no consensus regarding frequencies of systemic B cell subsets in pregnant women, healthy pregnancy, especially in its final stages, was consistently shown to be marked by a decrease in absolute numbers of circulating B cells (Bhat et al., 1995; Delgado et al., 1994; Kraus et al., 2012;

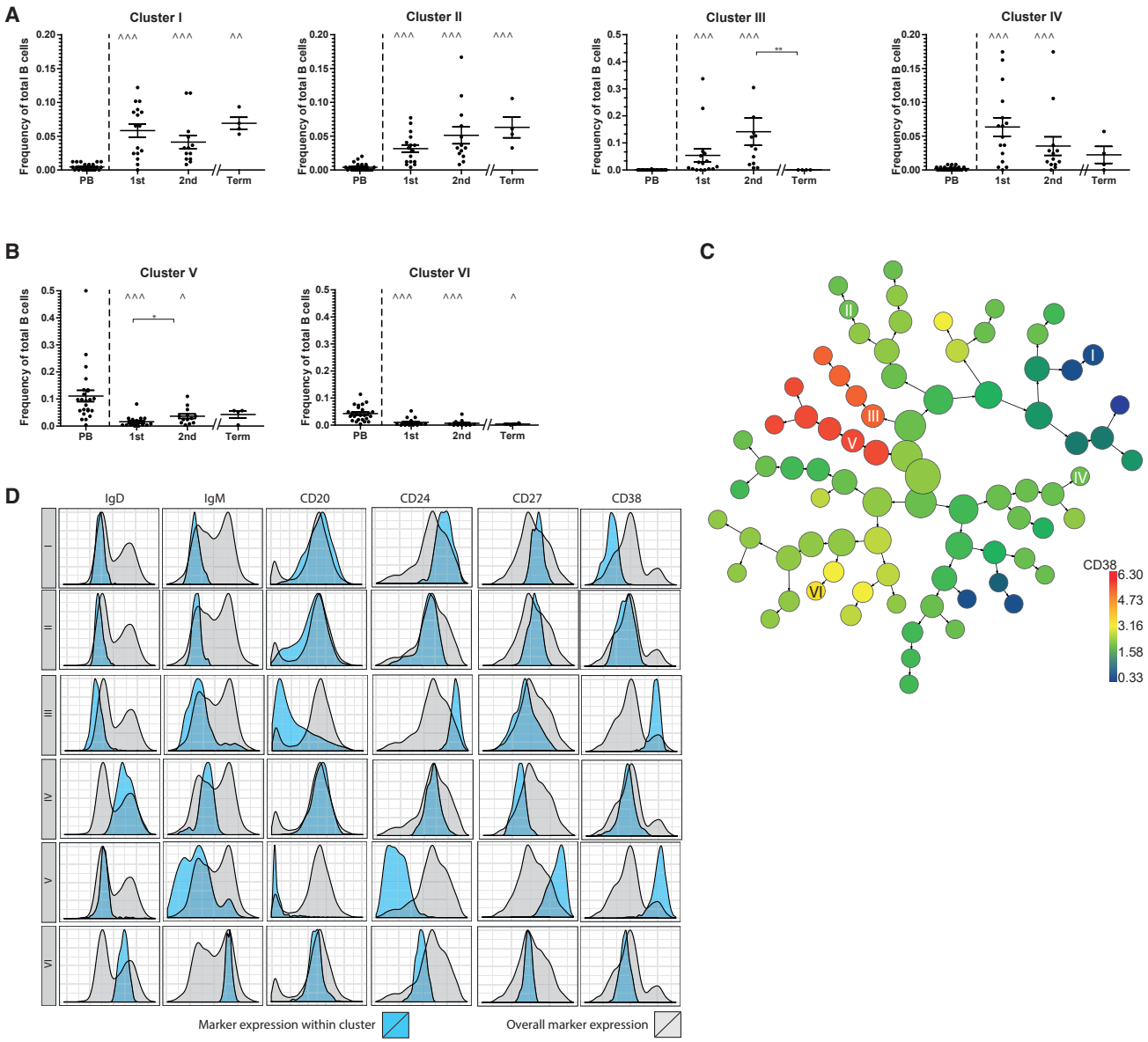

Figure 3. Unsupervised Clustering of B Cell Subsets in Decidua

(A and B) Decidual B cells (n = 33) were stratified by automatic clustering based on IgD, IgM, CD20, CD24, CD27, and CD38 expression using the CITRUS tool by Cytobank and compared with PB (n = 25). 246 B cells, as gated in Figure S3A for each sample, were used as input. A minimum cluster size of 2% was handled. Clusters of significantly higher expression (clusters I–IV, A) or lower expression (clusters V and VI, B) in decidua compared with PB are shown, and abundance was separated into the individual gestational time points. Abundance depicts the number of cells within a cluster divided by the total number of cells per sample. Samples of <200 B cells were excluded. 1st trimester, n = 16; 2nd trimester, n = 13; term, n = 4.

(C) Clustering tree depicting the relationships of identified clusters. The color scale illustrates relative marker expression per cluster, whereas the size of each node represents event frequency. As an example, CD38 expression is shown (remaining markers, Figure S3B).

(D) Marker expression of each subset in relation to overall expression.

^p < 0.05, ^^p < 0.01, ^^^p < 0.001, Kruskal-Wallis and Dunn's multiple-comparison tests; *p < 0.05, **p < 0.01 to compare 1st-trimester, 2nd-trimester, and term decidua. Data are represented as mean ± SEM.

Lima et al., 2016; Watanabe et al., 1997). This may be explained by a decrease in B cell lymphopoiesis, as was shown in mice during gestation (Medina et al., 1993; Muzzio et al., 2014), but it may also result from distribution to local sites. Our observation that naive B cells in early decidual tissues increase in abundance and switch to a memory phenotype could be an indication that redistribution occurs.

The question is, what purpose do these decidual B cells serve? Although there are indications that B cells may contribute to the inflammation required for the onset of labor (Gomez-Lopez

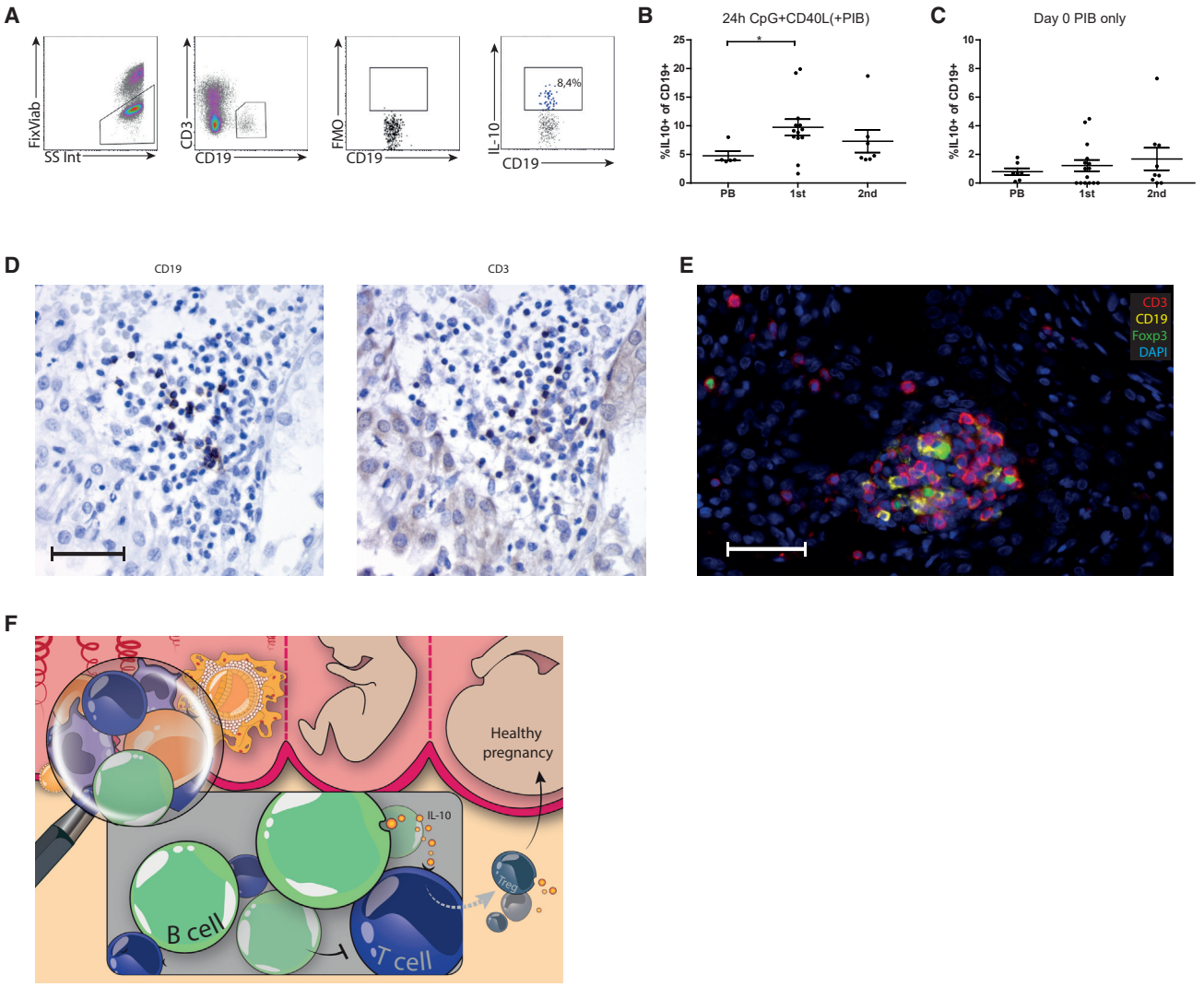

Figure 4. B Cells in Decidua Secrete IL-10

(A) Representative gating strategy for assessment of intracellular IL-10 in PB and decidual B cells. Live $CD19^{pos}$ events were selected. For each IL-10 assessment, a fluorescent-minus-one (FMO) strategy (using a staining mix excluding IL-10) was applied to cells subjected to the identical conditions for correct positioning of the gate selecting IL-10-positive cells.

(B) 50,000 mononuclear cells were stimulated for 24 h with 5 μg/mL of CpG and 1 μg/mL of CD40L or (C) in absence of stimulation. PB, n = 7; 1^{st} trimester, n = 15; 2^{nd} trimester, n = 9.

(D) Representative immunohistochemistry of 10-week decidua stained for CD19 (brown) and CD3 (red) of decidual lymphocyte clusters (n = 8 in 3 biological replicates, 9–14.5 weeks). Original magnification ×40, scale bar (black) indicating 200 μm.

(E) Representative 4-color multiplex staining of 10-week decidua. Original magnification ×20, scale bar (white) indicating 50 μm.

(F) Schematic representation summarizing colocalization of B and T cells. Decidual B cells are able to secrete IL-10, with a possible impact on Treg cell maintenance and thus healthy pregnancy.

PIB, phorbol-12-myristate-13-acetate + ionomycin + brefeldin A. **$p < 0.01$ Kruskal-Wallis and Dunn's multiple-comparison tests for comparison of PB and 1^{st}-trimester and 2^{nd}-trimester decidua. Data are shown as mean ± SEM.

et al., 2011), decidual B cells may serve an additional purpose. Through supervised and unsupervised analysis, we observed high frequencies of $CD24^{hi}CD27^{pos}$ (cluster I) and $CD24^{hi}CD38^{hi}$ (cluster III) B cells in 1^{st}- and 2^{nd}-trimester decidua, cell types associated with capacity for producing IL-10, a cytokine involved in immune regulation (Hasan et al., 2019). In our hands, decidual B cells produced IL-10 more than peripheral blood B cells, even without prior *in vitro* stimulation. The latter may suggest that decidual B cells already received the necessary activation *in utero*. Unsupervised analysis revealed that these cell clusters, together with two additional clusters expressing CD24 and CD38 (clusters II and IV), are unique for decidua and not present in peripheral blood. These cells might represent a specialized tissue-resident B cell subset, or they may be induced *de novo*

through local interaction with fetal cells. Indeed, recent *in vitro* experiments point out that trophoblast cells have the capacity to upregulate IL-10 in B cells, underlining the impact of fetal cells on B cell stimulation during the peri-implantation period (Guzman-Genuino et al., 2019a). Likewise, upon *in vitro* stimulation, B cells derived from 1st-trimester decidua produced IL-10. This might support the notion that B cell-mediated IL-10 production is induced relatively early in gestation, shortly after the primary encounter with invading fetal trophoblast cells. So far, there is only scant availability of data regarding decidual IL-10 expression *in vivo* (Hanna et al., 2000). Accordingly, by using immunohistochemistry, we found that *in vivo* IL-10-producing B cells were not readily detectable. IL-10 staining in tissues poses a technical challenge: IL-10 has a short half-life, it is rapidly secreted, and secreted levels *in vivo* in the local microenvironment, although functionally relevant, may likely be too low to yield positive staining results (Kamanaka et al., 2006). Although unsupervised clustering of decidual B cells did not show significant differences in subsets between the 1st and the 2nd trimesters, less IL-10 production upon *in vitro* stimulation of decidual immune cells was observed in the 2nd trimester. It may be possible that the potency of IL-10 production declines independent of the unchanged phenotype.

CD20 is a well-known marker expressed by multiple B cell subsets, among which are B cells with regulatory function (Blair et al., 2010). Unsupervised analysis showed that the most abundantly expressed B cell populations lacked CD20. Hasan and colleagues showed the diverse heterogeneity of marker expression by Breg cells, but unfortunately, they did not include CD20 in their study (Hasan et al., 2019). Although the biological function of CD20 remains poorly understood, future studies might benefit from considering CD20 as a differentially expressed marker.

We found that decidual B cells colocalized with T cells, similar to what has been described for non-pregnant endometrium (Yeaman et al., 1997). This colocalization supports the possibility of a functional interaction that may go both ways: T cell-derived cytokines may facilitate the induction of Breg cells (Rosser et al., 2014), whereas through the production of IL-10, Breg cells may contribute to the induction of Foxp3pos Treg cells (Blair et al., 2010; Flores-Borja et al., 2013; Rosser and Mauri, 2015). In decidua, we detected Foxp3pos T cells in clusters of lymphocytes located close to B cells. In healthy individuals, peripheral blood Breg cells convert effector T cells to Treg cells through IL-10 production and inhibit development of naive T cells toward Th1 or Th17 cells (Flores-Borja et al., 2013), thereby mediating suppression in case of a local inflammatory reaction (Rosser and Mauri, 2015). It is thus tempting to speculate that the IL-10 secreted by nearby B cells contributes to placental Treg cell induction and maintenance; these latter cells are well recognized for their contribution to successful pregnancy (Aluvihare et al., 2004; Saito et al., 2010). So, besides the idea that colocalization of decidual T and B cells is a phenomenon exclusive to pathologies (Novak et al., 1988), the interaction between Breg and T cells may just as well contribute to the required homeostasis and the tight regulation needed for healthy placentation while preserving immune competence at the fetal-maternal interface. Unfortunately, the low number of B cells that can be isolated per sample restricts experimental possibilities to assess their suppressive capacity on T cells. Even though their contribution in numbers within decidual lymphocytes is small, we propose that their effect might be amplified through proximity and effect on T cells and possible Treg cell induction (Figure 4E).

In conclusion, the current study highlights the complex dynamics of the human uterine immune landscape, including B cells with the potential to contribute to the immune-regulatory environment of the uterus during pregnancy.

STAR★METHODS

Detailed methods are provided in the online version of this paper and include the following:

- KEY RESOURCES TABLE
- RESOURCE AVAILABILITY
  - Lead Contact
  - Materials Availability
  - Data and Code Availability
- EXPERIMENTAL MODEL AND SUBJECT DETAILS
- METHOD DETAILS
  - Sample collection
  - Cell isolation
  - Flow cytometry staining and analysis
  - CITRUS clustering
  - B cell stimulation assays
  - Immunohistochemistry
- QUANTIFICATION AND STATISTICAL ANALYSIS

SUPPLEMENTAL INFORMATION

Supplemental Information can be found online at https://doi.org/10.1016/j.celrep.2020.108204.

ACKNOWLEDGMENTS

We thank all women who participated in this study and the staff of MildredHuis. We appreciate all help of Dr. Anita van der Zwan for helpful discussions to optimize placenta dissociation for phenotyping, Daan Zegers during processing, and Niklas Bruse and Rindert Hartman for assistance in data formatting. M.B. is supported by a junior researcher grant of the Radboud Institute for Molecular Life Sciences.

AUTHOR CONTRIBUTIONS

Conceptualization, M.B., G.F., I.J., and R.G.v.d.M.; Methodology, M.B., D.F., C.C.G., and N.I.; Formal Analysis, M.B., C.C.G., and N.I.; Investigation, M.B., D.F., C.C.G., N.I., S.C.L., E.F., and M.A.J.G.; Writing – Original Draft, M.B., D.F., G.F., I.J., and R.G.v.d.M.; Writing – Review & Editing, M.B., D.F., G.F., I.J., and R.G.v.d.M.; Visualization, M.B.; Funding Acquisition, I.J. and R.G.v.d.M.; Resources, W.S. and O.W.H.v.d.H.; Supervision, G.F., R.G.v.d.M., and I.J.

DECLARATION OF INTERESTS

The authors declare no competing interests.

Received: October 31, 2019
Revised: July 16, 2020
Accepted: September 4, 2020
Published: September 29, 2020

REFERENCES

Aghaeepour, N., Ganio, E.A., Mcilwain, D., Tsai, A.S., Tingle, M., Van Gassen, S., Gaudilliere, D.K., Baca, Q., McNeil, L., Okada, R., et al. (2017). An immune clock of human pregnancy. Sci. Immunol. *2*, eaan2946.

Aluvihare, V.R., Kallikourdis, M., and Betz, A.G. (2004). Regulatory T cells mediate maternal tolerance to the fetus. Nat. Immunol. *5*, 266–271.

Ashdown, H., Dumont, Y., Ng, M., Poole, S., Boksa, P., and Luheshi, G.N. (2006). The role of cytokines in mediating effects of prenatal infection on the fetus: implications for schizophrenia. Mol. Psychiatry *11*, 47–55.

Bhat, N.M., Mithal, A., Bieber, M.M., Herzenberg, L.A., and Teng, N.N. (1995). Human CD5+ B lymphocytes (B-1 cells) decrease in peripheral blood during pregnancy. J. Reprod. Immunol. *28*, 53–60.

Blair, P.A., Noreña, L.Y., Flores-Borja, F., Rawlings, D.J., Isenberg, D.A., Ehrenstein, M.R., and Mauri, C. (2010). CD19(+)CD24(hi)CD38(hi) B cells exhibit regulatory capacity in healthy individuals but are functionally impaired in systemic Lupus Erythematosus patients. Immunity *32*, 129–140.

Bright, P., Grigoriadou, S., Kamperidis, P., Buckland, M., Hickey, A., and Longhurst, H.J. (2013). Changes in B cell immunophenotype in common variable immunodeficiency: cause or effect—is bronchiectasis indicative of undiagnosed immunodeficiency? Clin. Exp. Immunol. *171*, 195–200.

Bruggner, R.V., Bodenmiller, B., Dill, D.L., Tibshirani, R.J., and Nolan, G.P. (2014). Automated identification of stratifying signatures in cellular subpopulations. Proc. Natl. Acad. Sci. USA *111*, E2770–E2777.

Busse, M., Campe, K.J., Nowak, D., Schumacher, A., Plenagl, S., Langwisch, S., Tiegs, G., Reinhold, A., and Zenclussen, A.C. (2019). IL-10 producing B cells rescue mouse fetuses from inflammation-driven fetal death and are able to modulate T cell immune responses. Sci. Rep. *9*, 9335.

Carbone, J., Sarmiento, E., Gallego, A., Lanio, N., Navarro, J., García, S., and Fernandez-Cruz, E. (2016). Peripheral blood T- and B-cell immunophenotypic abnormalities in selected women with unexplained recurrent miscarriage. J. Reprod. Immunol. *113*, 50–53.

Carter, N.A., Vasconcellos, R., Rosser, E.C., Tulone, C., Muñoz-Suano, A., Kamanaka, M., Ehrenstein, M.R., Flavell, R.A., and Mauri, C. (2011). Mice lacking endogenous IL-10-producing regulatory B cells develop exacerbated disease and present with an increased frequency of Th1/Th17 but a decrease in regulatory T cells. J. Immunol. *186*, 5569–5579.

Daien, C.I., Gailhac, S., Mura, T., Audo, R., Combe, B., Hahne, M., and Morel, J. (2014). Regulatory B10 cells are decreased in patients with rheumatoid arthritis and are inversely correlated with disease activity. Arthritis Rheumatol. *66*, 2037–2046.

Delgado, I., Neubert, R., and Dudenhausen, J.W. (1994). Changes in white blood cells during parturition in mothers and newborn. Gynecol. Obstet. Invest. *38*, 227–235.

Dimitriadis, E., White, C.A., Jones, R.L., and Salamonsen, L.A. (2005). Cytokines, chemokines and growth factors in endometrium related to implantation. Hum. Reprod. Update *11*, 613–630.

Dutta, S., Sengupta, P., and Haque, N. (2019). Reproductive immunomodulatory functions of B cells in pregnancy. Int. Rev. Immunol. *39*, 53–66.

Feyaerts, D., Benner, M., van Cranenbroek, B., van der Heijden, O.W.H., Joosten, I., and van der Molen, R.G. (2017). Human uterine lymphocytes acquire a more experienced and tolerogenic phenotype during pregnancy. Sci. Rep. *7*, 2884.

Feyaerts, D., Kuret, T., van Cranenbroek, B., van der Zeeuw-Hingrez, S., van der Heijden, O.W.H., van der Meer, A., Joosten, I., and van der Molen, R.G. (2018). Endometrial natural killer (NK) cells reveal a tissue-specific receptor repertoire. Hum. Reprod. *33*, 441–451.

Flores-Borja, F., Bosma, A., Ng, D., Reddy, V., Ehrenstein, M.R., Isenberg, D.A., and Mauri, C. (2013). CD19+CD24hiCD38hi B cells maintain regulatory T cells while limiting TH1 and TH17 differentiation. Sci. Transl. Med. *5*, 173ra23.

Gamliel, M., Goldman-Wohl, D., Isaacson, B., Gur, C., Stein, N., Yamin, R., Berger, M., Grunewald, M., Keshet, E., Rais, Y., et al. (2018). Trained Memory of Human Uterine NK Cells Enhances Their Function in Subsequent Pregnancies. Immunity *48*, 951–962.

Gomez-Lopez, N., Vadillo-Perez, L., Nessim, S., Olson, D.M., and Vadillo-Ortega, F. (2011). Choriodecidua and amnion exhibit selective leukocyte chemotaxis during term human labor. Am. J. Obstet. Gynecol. *204*, 364.e9-16.

Guzman-Genuino, R.M., and Diener, K.R. (2017). Regulatory B Cells in Pregnancy: Lessons from Autoimmunity, Graft Tolerance, and Cancer. Front. Immunol. *8*, 172.

Guzman-Genuino, R.M., Dimova, T., You, Y., Aldo, P., Hayball, J.D., Mor, G., and Diener, K.R. (2019a). Trophoblasts promote induction of a regulatory phenotype in B cells that can protect against detrimental T cell-mediated inflammation. Am. J. Reprod. Immunol. *82*, e13187.

Guzman-Genuino, R.M., Eldi, P., Garcia-Valtanen, P., Hayball, J.D., and Diener, K.R. (2019b). Uterine B Cells Exhibit Regulatory Properties During the Peri-Implantation Stage of Murine Pregnancy. Front. Immunol. *10*, 2899.

Han, X., Ghaemi, M.S., Ando, K., Peterson, L.S., Ganio, E.A., Tsai, A.S., Gaudilliere, D.K., Stelzer, I.A., Einhaus, J., Bertrand, B., et al. (2019). Differential Dynamics of the Maternal Immune System in Healthy Pregnancy and Preeclampsia. Front. Immunol. *10*, 1305.

Hanna, N., Hanna, I., Hleb, M., Wagner, E., Dougherty, J., Balkundi, D., Padbury, J., and Sharma, S. (2000). Gestational age-dependent expression of IL-10 and its receptor in human placental tissues and isolated cytotrophoblasts. J. Immunol. *164*, 5721–5728.

Hasan, M.M., Thompson-Snipes, L., Klintmalm, G., Demetris, A.J., O'Leary, J., Oh, S., and Joo, H. (2019). $CD24^{hi}CD38^{hi}$ and $CD24^{hi}CD27^{+}$ Human Regulatory B Cells Display Common and Distinct Functional Characteristics. J. Immunol. *203*, 2110–2120.

Hosseini, S., Zarnani, A.-H., Asgarian-Omran, H., Vahedian-Dargahi, Z., Eshraghian, M.R., Akbarzadeh-Pasha, Z., Arefi, S., Jeddi-Tehrani, M., and Shokri, F. (2014). Comparative analysis of NK cell subsets in menstrual and peripheral blood of patients with unexplained recurrent spontaneous abortion and fertile subjects. J. Reprod. Immunol. *103*, 9–17.

Hsu, P., and Nanan, R. (2014). Foetal immune programming: hormones, cytokines, microbes and regulatory T cells. J. Reprod. Immunol. *104–105*, 2–7.

Iwata, Y., Matsushita, T., Horikawa, M., Dilillo, D.J., Yanaba, K., Venturi, G.M., Szabolcs, P.M., Bernstein, S.H., Magro, C.M., Williams, A.D., et al. (2011). Characterization of a rare IL-10-competent B-cell subset in humans that parallels mouse regulatory B10 cells. Blood *117*, 530–541.

Kamanaka, M., Kim, S.T., Wan, Y.Y., Sutterwala, F.S., Lara-Tejero, M., Galán, J.E., Harhaj, E., and Flavell, R.A. (2006). Expression of interleukin-10 in intestinal lymphocytes detected by an interleukin-10 reporter knockin tiger mouse. Immunity *25*, 941–952.

Klein, U., Rajewsky, K., and Küppers, R. (1998). Human immunoglobulin (Ig) M+IgD+ peripheral blood B cells expressing the CD27 cell surface antigen carry somatically mutated variable region genes: CD27 as a general marker for somatically mutated (memory) B cells. J. Exp. Med. *188*, 1679–1689.

Kotecha, N., Krutzik, P.O., and Irish, J.M. (2010). Web-based analysis and publication of flow cytometry experiments. Curr. Protoc. Cytom. *53*, 10.17.1–10.17.24.

Kralickova, P., Kurecova, B., Andrys, C., Krcmova, I., Jilek, D., Vlkova, M., and Litzman, J. (2015). Pregnancy Outcome in Patients with Common Variable Immunodeficiency. J. Clin. Immunol. *35*, 531–537.

Kraus, T.A., Engel, S.M., Sperling, R.S., Kellerman, L., Lo, Y., Wallenstein, S., Escribese, M.M., Garrido, J.L., Singh, T., Loubeau, M., and Moran, T.M. (2012). Characterizing the pregnancy immune phenotype: results of the viral immunity and pregnancy (VIP) study. J. Clin. Immunol. *32*, 300–311.

Lasala, N., and Zhou, H. (2007). Effects of maternal exposure to LPS on the inflammatory response in the offspring. J. Neuroimmunol. *189*, 95–101.

Lima, J., Martins, C., Leandro, M.J., Nunes, G., Sousa, M.-J., Branco, J.C., and Borrego, L.-M. (2016). Characterization of B cells in healthy pregnant women from late pregnancy to post-partum: a prospective observational study. BMC Pregnancy Childbirth *16*, 139.

Medina, K.L., Smithson, G., and Kincade, P.W. (1993). Suppression of B lymphopoiesis during normal pregnancy. J. Exp. Med. *178*, 1507–1515.

Mitchell, B.F., and Taggart, M.J. (2009). Are animal models relevant to key aspects of human parturition? Am. J. Physiol. Regul. Integr. Comp. Physiol. *297*, R525–R545.

Mor, G., Cardenas, I., Abrahams, V., and Guller, S. (2011). Inflammation and pregnancy: the role of the immune system at the implantation site. Ann. N Y Acad. Sci. *1221*, 80–87.

Muzzio, D.O., Soldati, R., Ehrhardt, J., Utpatel, K., Evert, M., Zenclussen, A.C., Zygmunt, M., and Jensen, F. (2014). B cell development undergoes profound modifications and adaptations during pregnancy in mice. Biol. Reprod. *91*, 115.

Novak, R., Agamanolis, D., Dasu, S., Igel, H., Platt, M., Robinson, H., and Shehata, B. (1988). Histologic analysis of placental tissue in first trimester abortions. Pediatr. Pathol. *8*, 477–482.

Ota, K., Dambaeva, S., Lee, J., Gilman-Sachs, A., Beaman, K., and Kwak-Kim, J. (2014). Persistent high levels of IgM antiphospholipid antibodies in a patient with recurrent pregnancy losses and rheumatoid arthritis. Am. J. Reprod. Immunol. *71*, 286–292.

Pavlasova, G., and Mraz, M. (2020). The regulation and function of CD20: an "enigma" of B-cell biology and targeted therapy. Haematologica *105*, 1494–1506.

Ratnayake, U., Quinn, T., Walker, D.W., and Dickinson, H. (2013). Cytokines and the neurodevelopmental basis of mental illness. Front. Neurosci. *7*, 180.

Redman, C.W.G., and Sargent, I.L. (2010). Immunology of pre-eclampsia. Am. J. Reprod. Immunol. *63*, 534–543.

Robertson, S.A., and Moldenhauer, L.M. (2014). Immunological determinants of implantation success. Int. J. Dev. Biol. *58*, 205–217.

Robertson, S.A., Chin, P.Y., Glynn, D.J., and Thompson, J.G. (2011). Peri-conceptual cytokines—setting the trajectory for embryo implantation, pregnancy and beyond. Am. J. Reprod. Immunol. *66* (*Suppl 1*), 2–10.

Rosser, E.C., and Mauri, C. (2015). Regulatory B cells: origin, phenotype, and function. Immunity *42*, 607–612.

Rosser, E.C., Oleinika, K., Tonon, S., Doyle, R., Bosma, A., Carter, N.A., Harris, K.A., Jones, S.A., Klein, N., and Mauri, C. (2014). Regulatory B cells are induced by gut microbiota-driven interleukin-1beta and interleukin-6 production. Nature Medicine *20*, 1334–1339.

Saito, S., Nakashima, A., Shima, T., and Ito, M. (2010). Th1/Th2/Th17 and regulatory T-cell paradigm in pregnancy. Am. J. Reprod. Immunol. *63*, 601–610.

Sanz, I., Wei, C., Lee, F.E.-H., and Anolik, J. (2008). Phenotypic and functional heterogeneity of human memory B cells. Semin. Immunol. *20*, 67–82.

Sarvaria, A., Madrigal, J.A., and Saudemont, A. (2017). B cell regulation in cancer and anti-tumor immunity. Cell. Mol. Immunol. *14*, 662–674.

Shynlova, O., Lee, Y.-H., Srikhajon, K., and Lye, S.J. (2013a). Physiologic uterine inflammation and labor onset: integration of endocrine and mechanical signals. Reprod. Sci. *20*, 154–167.

Shynlova, O., Nedd-Roderique, T., Li, Y., Dorogin, A., and Lye, S.J. (2013b). Myometrial immune cells contribute to term parturition, preterm labour and post-partum involution in mice. J. Cell. Mol. Med. *17*, 90–102.

Simon, Q., Pers, J.-O., Cornec, D., Le Pottier, L., Mageed, R.A., and Hillion, S. (2016). In-depth characterization of CD24(high)CD38(high) transitional human B cells reveals different regulatory profiles. J. Allergy Clin. Immunol. *137*, 1577–1584.

Slawek, A., Lorek, D., Kedzierska, A.E., and Chelmonska-Soyta, A. (2020). Regulatory B cells with IL-35 and IL-10 expression in a normal and abortion-prone murine pregnancy model. Am. J. Reprod. Immunol. *83*, e13217.

Smith, G.C. (2010). First-trimester determination of complications of late pregnancy. JAMA *303*, 561–562.

Tao, Y., Li, Y.-H., Piao, H.-L., Zhou, W.-J., Zhang, D., Fu, Q., Wang, S.-C., Li, D.-J., and Du, M.-R. (2015). CD56(bright)CD25+ NK cells are preferentially recruited to the maternal/fetal interface in early human pregnancy. Cell. Mol. Immunol. *12*, 77–86.

Tsuda, S., Nakashima, A., Shima, T., and Saito, S. (2019). New Paradigm in the Role of Regulatory T Cells During Pregnancy. Front. Immunol. *10*, 573.

Watanabe, M., Iwatani, Y., Kaneda, T., Hidaka, Y., Mitsuda, N., Morimoto, Y., and Amino, N. (1997). Changes in T, B, and NK lymphocyte subsets during and after normal pregnancy. Am. J. Reprod. Immunol. *37*, 368–377.

Xing, C., Ma, N., Xiao, H., Wang, X., Zheng, M., Han, G., Chen, G., Hou, C., Shen, B., Li, Y., and Wang, R. (2015). Critical role for thymic CD19+CD5+CD1dhiIL-10+ regulatory B cells in immune homeostasis. J. Leukoc. Biol. *97*, 547–556.

Xu, Y., Plazyo, O., Romero, R., Hassan, S.S., and Gomez-Lopez, N. (2015). Isolation of Leukocytes from the Human Maternal-fetal Interface. J. Vis. Exp. *99*, e52863.

Yeaman, G.R., Guyre, P.M., Fanger, M.W., Collins, J.E., White, H.D., Rathbun, W., Orndorff, K.A., Gonzalez, J., Stern, J.E., and Wira, C.R. (1997). Unique CD8+ T cell-rich lymphoid aggregates in human uterine endometrium. Journal of Leukocyte Biology *61*, 427–435.

Zeng, B., Kwak-Kim, J., Liu, Y., and Liao, A.-H. (2013). Treg cells are negatively correlated with increased memory B cells in pre-eclampsia while maintaining suppressive function on autologous B-cell proliferation. Am. J. Reprod. Immunol. *70*, 454–463.

STAR★METHODS

KEY RESOURCES TABLE

REAGENT or RESOURCE	SOURCE	IDENTIFIER
Antibodies		
AE1/3, opal650; AE1/AE3 + 5D3	Abcam	RRID:AB_1067432, Cat #ab86734
CD3, AP-red; F7.2.38	Abcam	RRID:AB_302587, Cat #ab17143
CD3, PB; UCHT1	Beckman Coulter	Cat #B49204
CD3, PE; UCHT1	Beckman Coulter	Cat #A07747
CD3, ECD; UCHT1	Beckman Coulter	Cat #A07748
CD3, opal520, sp7	ThermoFisher	RRID:AB_1956722, Cat #MA1-90582
CD4, PE-Cy5.5; 13B8.2	Beckman Coulter	Cat #B16491
CD4, PB; 13B8.2	Beckman Coulter	Cat #B49197
CD4, AF700; RPA-T4	eBioscience	RRID:AB_11219085, Cat #56-0049-42
CD5, APC-AF700; BL1a	Beckman Coulter	Cat #A78835
CD8, APC-AF700; B9.11	Beckman Coulter	Cat #B49181
CD8, APC-AF750; B9.11	Beckman Coulter	Cat #A94683
CD8, ECD; SFCI21Thy2D3	Beckman Coulter	RRID:AB_2751015, Cat #737659
CD8, opal690; C8/144B	Dako	RRID:AB_1280806, Cat #ab75129
CD14, ECD; RMO52	Beckman Coulter	Cat #IM2707U
CD16, FITC; DJ130c	Beckman Coulter	Cat #B49215
CD19, APC-AF750; J3-119	Beckman Coulter	RRID:AB_2833030, Cat #A94681
CD19, DAB; EPR5906	Abcam	RRID:AB_2801636, Cat #ab134114
CD19, opal570; EPR5906	Abcam	RRID:AB_2801636, Cat # ab134114
CD20, PB; B9E9	Beckman Coulter	Cat #A74777
CD24, APC; ALB9	Beckman Coulter	Cat #A87785
CD25, PC7; M-A251	BD	RRID:AB_396847, Cat #557741
CD25, APC; M-A251	BD	RRID:AB_2819021, Cat #340907
CD27, PE-Cy5.5; BC96	Beckman Coulter	Cat #B21444
CD38, PC7; LS198-4-3	Beckman Coulter	Cat #B49198
CD45, KO; J33	Beckman Coulter	RRID:AB_2833027, Cat #B36294
CD45, ECD; J33	Beckman Coulter	Cat #A07784
CD45RA, FITC; ALB11	Beckman Coulter	Cat #A07786
CD45RA, ECD; 2H4LDH11LDB9	Beckman Coulter	Cat #B49193
CD56, APC; N901(NKH-1)	Beckman Coulter	RRID:AB_130791, Cat #IM2474
CD56, opal620; MRQ-42	Cell Marque	Cat #156R-94
CD127, APC-750; R34.34	Beckman Coulter	Cat #A71116
CD183, PerCp5.5; G025H7	Biolegend	RRID:AB_10962908, Cat #353714
CD194, PE-Cy7; 1G1	BD	RRID:AB_396907, Cat #557864
CD195, APC-Cy7; 2D7	BD	RRID:AB_396861, Cat #557755
CD196, PE; 11A9	BD	RRID:AB_397273, Cat #559562
CD197, BV421; G043H7	Biolegend	RRID:AB_11203894, Cat #353208
Foxp3, e450; PCH101	eBiocience	RRID:AB_1834364, Cat #48-4776-42
Foxp3, opal540; 236A/E7	eBioscience/Affymetrix	RRID:AB_467556, Cat #14-4777-82
Helios, AF647; 22F6	Biolegend	RRID:AB_10660750, Cat #137218
HLA-DR, PE; Immu-357	Beckman Coulter	Cat #IM1639U
IgD, FITC; IADB6	Beckman Coulter	Cat #735993
IgM, PE; SA-DA4	Beckman Coulter	Cat #735951

(*Continued on next page*)

Continued

REAGENT or RESOURCE	SOURCE	IDENTIFIER
IL-10, PE; JES3-19F1	Biolegend	RRID:AB_315454, Cat #506804
KI67, AF488; B56	BD	RRID:AB_10611866, Cat #561165
FixViab, eFluor 780	eBioscience	Cat #65-0865-14
Biological Samples		
Human decidual and placental tissue (from 4.7-17.3 week gestation elective terminations)	Local reproductive health clinic	N/A
Human term placental tissue (> 37weeks gestation; from planned cesarean section following uncomplicated pregnancy)	Radboud University Medical Center	N/A
Healthy donor peripheral blood and menstrual blood donations	Radboud University Medical Center	N/A
Chemicals, Peptides, and Recombinant Proteins		
Accutase	GIBCO	Cat #A11105-01
Brefeldin A	Sigma-Aldrich	Cat #B7651
Collagenase type IV	GIBCO Life Technologies	Cat #C5138
DNase I	Roche Diagnostics	Cat #DN25
Ionomycin	Sigma Aldrich	Cat # 10634
Ficoll Lymphoprep	Axis-Shield	Cat# 07861
Percoll	GE Healthcare	Cat #17-0891-01
phorbol-12-myristate-13-acetate	Sigma Aldrich	Cat #16561-29-8
Recombinant human CD40L	Shenandoah Biotechnology	SHBT100-25AF
Critical Commercial Assays		
CytoFix/CytoPerm intracellular staining kit	eBioscience	Cat #00-5523-00
Fluoromount-G	SouthernBiotech	Cat #0100-01
gentleMACS dissociation system	Miltenyi Biotec GmbH	https://www.miltenyibiotec.com/US-en/products/
Human granulocyte depletion cocktail RosetteSep	Stemcell technologies Inc	Cat #15624
Opal seven-color IHC Kit	Akoya Biosciences	Cat #NEL797B001KT
Oligonucleotides		
ODN 2006 CpG	Hycult Biotech	Cat #HC4039
Software and Algorithms		
Cytobank	Cytobank	https://www.cytobank.org/
GraphPad Prism 5	GraphPad Prism	https://www.graphpad.com/scientific-software/prism/
inForm software (Version 2.4.8)	Akoya Biosciences	https://akoyabio.helpdocs.com/phenoptics-software-updates/inform-248
Kaluza (Version 1.3 and 2.1)	Beckman Coulter	https://www.mybeckman.nl/flow-cytometry/software/kaluza
R plugin for Kaluza fcs export	Beckman Coulter	Benoit Dupont

RESOURCE AVAILABILITY

Lead Contact

Further information and requests for resources and reagents should be directed to and will be fulfilled by the Lead Contact, Renate van der Molen (renate.vandermolen@radboudumc.nl).

Materials Availability

This study did not generate new unique reagents.

Data and Code Availability

The published article includes all datasets generated during this study. Raw flow cytometry data are available upon request.

EXPERIMENTAL MODEL AND SUBJECT DETAILS

Peripheral blood was collected from 36 healthy female volunteers (mean age 22.8 years ± 3.4 years). Exclusion criteria were smoking, chronic disease, medication, carrier of an infectious disease and pregnancy. Menstrual blood was provided by 28 healthy women (exclusion criteria: known fertility disorder, potential carrier of an infectious disease, auto-immune disease, drug abuse, or use of hormonal or intra-uterine device contraceptives) with regular menstrual cycle. First and 2nd trimester material was obtained from discarded placental and decidual tissue upon elective pregnancy termination of healthy women at a local reproductive health clinic. No additional data other than gestational age at time point of termination was acquired. Exclusion criteria were carrier of an infectious disease (active systemic infection), suspected to be a potential carrier of an infectious disease or an increased risk for infection (HIV, Hep B/C, HTLV or similar), auto-immune diseases, drug abuse, intoxication with heavy metals or pesticides. Term placental tissue (> 37weeks gestation) was collected from planned cesarean section following uncomplicated pregnancy. Exclusion criteria were gestational age < 37 weeks, use of immunosuppressive drugs, biological or antidepressants, HIV positivity, active infection during caesarean section, signs of infection (maternal fever or signs of intrauterine infection), use of antibiotics prior to caesarean section. All gestational samples were assessed visually and excluded for processing in case of signs of infection (discoloration) or excessive blood clots. Written informed consent was obtained for all volunteers donating blood or tissue for this study in accordance with the Dutch Medical Research Involving Human Subject Act (WMO). The study was approved by the local review board (Commissie Mensgebonden Onderzoek region Arnhem-Nijmegen, 42561.091.12, 2017-3253, 2014-232, 2009/004). An overview of all study participants is given in Table S1. The amount of individual participants included per experiment is indicated in the according legend as the amount of cells isolated per sample limited the number of experiments carried out simultaneously.

METHOD DETAILS

Sample collection

Peripheral blood was collected using EDTA tubes. For menstrual blood, women were asked to use a menstrual cup (Femmecup Ltd, London, UK) and collect its content every 12h during the first 36h after initiation of menstruation. Contents of the cup were poured in a 30 mL tube containing 10 mL of supplemented RPMI 1640 medium (1 mM pyruvate, 2 mM glutamax, 100 U/ml penicillin, 100 μg/ml streptomycin (all Thermo Fisher Scientific Waltham, USA) 0.3% v/v sodium citrate (Merck Darmstadt, Germany) 10% v/v human pooled serum; HPS, manufactured in-house) for storage at room temperature until processing. After collection, menstrual blood samples were transferred to the lab immediately to undergo processing within max. 24h. First and second trimester tissue was transported to the lab at room temperature and processed immediately upon arrival.

Cell isolation

Flow cytometry staining was performed on either whole blood or, for Treg staining, on isolated mononuclear cell populations. Peripheral blood mononuclear cells were isolated from whole blood based on density gradient separation (1.077 ± 0.001 g/ml, 290 ± 15mOsm, Lymphoprep, Axis-Shield, Oslo, Norway). Menstrual blood mononuclear cells were isolated following an established protocol (Feyaerts et al., 2018; Gamliel et al., 2018). This protocol typically results in cell viability of ~96%. In brief, menstrual blood was washed with PBS (Braun, Melsungen, Germany) and filtered (70 μm cell strainer Falcon®, Corning Inc., NY, USA) to remove clots or excess mucus. A granulocyte depletion cocktail RosetteSep (Stemcell technologies Inc, Vancouver, Canada) was used according to manufacturer's instructions. After sterile density gradient centrifugation (Lymphoprep), menstrual blood mononuclear cells (MMC) were collected. First and 2nd trimester decidual leucocytes were isolated from maternal mucosal tissue that was carefully selected during visual assessment of the individual tissue pieces. Villous tissue, blood clots, glands and areas of blood infiltration were discarded. At these early stages of gestation, the selected pieces of membrane do not contain fused fetal membranes yet. Tissue pieces were minced mechanically using scissors and washed in PBS until the supernatant became transparent. For cells used for phenotyping, tissue was transferred to c-tubes (gentleMACS system) for additional mechanic processing using a MACS dissociator (Miltenyi Biotec GmbH, Bergisch Gladbach, Germany) prior to incubation with Accutase (Stempro, GIBCO Life Technologies, Waltham, USA) in a 1:2 tissue to enzyme ratio; a gentle dissociation method to preserve marker expression (Xu et al., 2015). For B cell assays, washed tissue was digested using 0.2% collagenase (GIBCO Life Technologies, Waltham, USA) and 0.04% DNase (Roche Diagnostics, Risch-Rotkreuz, Switzerland). Tissue digestion was performed in a shaking water bath at 37°C for 45 minutes. After digestion, the solution was filtered through 100 μm, 70 μm and 40 μm cell strainers consecutively. Lymphocytes were obtained through density gradient centrifugation by diluting the washed filtrate in 20 mL 1.023 g/ml Percoll (GE Healthcare, Little Chalfont, UK) to be layered on gradient of 10 mL 1.080 g/ml and 15ml 1.053 g/ml Percoll (centrifugation for 25min at 2000rpm). Large cells accumulating at the 1.053 – 1.023 g/ml interface were discarded and decidual leucocytes were isolated from the 1.080 – 1.053 g/ml interface. Leucocytes were washed twice in RPMI before further use. For term decidua, decidua parietalis was separated from the two fetal layers. The amnion was removed prior to scraping decidua parietalis from the chorionic membrane. After this, the isolation procedure was identical to that of 1st and 2nd trimester.

Flow cytometry staining and analysis

For whole blood staining, 25ml red blood cell lysis buffer [NH4CL + KHCO3/ Na4EDTA (Merck, Darmstadt, Germany) diluted in H_2O (Versol, Lyon, France)] was added to 1ml of peripheral blood for 10 min, and washed 3times with PBS. A minimum of 200.000 cells was used for staining with fluorochrome-conjugated monoclonal antibodies (moAbs) of interest for 20 min at RT in the dark. For Treg subset characterization and chemokine markers assessment a minimum of 500.000 mononuclear cells were used; 50.000 for intracellular cytokine assessment. For intracellular staining, fixation and permeabilization was carried out according to manufacturer's instructions (eBioscience, San Diego, USA). IL-10 detection was preceded by incubation with Fixable Viability Dye-eFluor 780/Krome Orange (eBioscience) in PBS for 30min at 4°C in the dark. Samples were measured using a 10-color Navios flow cytometer (Beckman Coulter, Fullerton, CA, USA). For manual gating, data were analyzed using Kaluza V2.1 (Beckman Coulter). Gates were set based on isotype controls and a fluorescent-minus-one strategy. Locations of gates were fixed except for CD3/CD56 based selection of NK cells as shown in Figure S1. A detailed gating strategy for the various cell subsets and tissue types is shown in Figure S1B.

CITRUS clustering

For unsupervised analysis, manually gated lymphocytes (Figure 1) or CD3 negative lymphocytes (for B cell analysis in Figure 3) were extracted (plug in provided by Beckman Coulter) before further processing using the web-based analysis platform Cytobank (http://cytobank.org/) (Kotecha et al., 2010). Lymphocytes and $CD19^{pos}$ B cells, respectively, were chosen as input population. Files were assigned to the appropriate gestational-age group, i.e., menstrual blood, 1st trimester, 2^{nd} trimester and term. Unsupervised clustering of lymphocyte and B cell frequencies was performed using the CITRUS tool. Clustering was performed based on abundance with a minimum cluster size of 2% of total cells and a false discovery rate of 1%. For B cell clustering, samples of less than 200 B cell events were excluded from analysis (lowest amount of events included was 246). Clustering was analyzed with prediction analysis for microarrays (PAM), a predictive model to identify features determining gestational age-dependent variation. Statistics associated with all identified clusters related to Figure 3 are shown in Data S1.

B cell stimulation assays

50.000 peripheral blood mononuclear cells or decidual lymphocytes were cultured in the presence or absence of CpG (5μg/ml) and CD40L (1μg/ml) stimulation, in 10% HPS culture media (RPMI 1640 medium supplemented with 1 mM pyruvate, 2 mM glutamax, 100 U/ml penicillin, and 100 μg/ml streptomycin) in a 96-well U-bottom plate for 24h at 37°C in a humidified 5% CO2 incubator. Phorbol-12-myristate-13-acetate (PMA, 50 ng/ml) and ionomycin (1 ug/ml) were added for the final 5h and brefeldin A (5μg/ml; Sigma-Aldrich, St. Louis, USA) for the final 2h of incubation. IL-10 expression of viable B cells was measured by flow cytometry as described.

Immunohistochemistry

Tissue samples were fixed in neutral buffered 4% formalin (Mallinckrodt Baker Inc, Deventer, the Netherlands) for 4h, transferred to 70% ethanol before preparation in a Tissue-Tek VIP tissue processor for embedding in paraffin. Slides were deparaffinized in xylene before rehydration, washing in tap water and boiling in Tris-EDTA buffer (pH 9, Klinipath). 6 μm sections were stained for either IHC or IF staining. For IHC staining, antibody binding was visualized by diaminobenzidine (Thermo Scientific) or Poly-HRP-goat-anti-mouse/rabbit/rat IgG (BrightVision, Duiven, the Netherlands) with permanent red. IHC staining was assessed microscopically (AxioImager M2; Zeiss, Sliedrecht, the Netherlands) and sections were photographed using a high resolution color camera for bright field microscopy (AxioCam 105 color, Zeiss). Images were assessed using ZEN blue edition version 2.3 (Zeiss). For IF staining, visualization was performed using the Opal seven-color IHC Kit (Akoya Biosciences) on the BOND RX IHC & ISH Research Platform (Leica Biosystems). All staining cycles contained heating steps in between cycles. Tissue sections were counterstained with DAPI and mounted in Fluoromount-G (SouthernBiotech). Images of stained slides were acquired using the Vectra (Vectra 3.0.4, PerkinElmer) and exported with inForm software (Version 2.4.8, Akoya Biosciences).

QUANTIFICATION AND STATISTICAL ANALYSIS

All statistical analysis was performed using GraphPad Prism 5 (La Jolla, CA, USA). All values represent mean percentages ± SEM (error bars). Kruskal-Wallis and post hoc Dunn's multiple comparison test (non-parametric) were performed to assess differences between mucosal isolates compared to peripheral blood as well as when assessing differences between mucosal tissues. Details on sample size and statistical outcomes can be found in the respective figure legends.